Current Medical Science
DOI https://doi.org/10.1007/s11596-023-2713-x
43(2):336-343,2023

Development and Validation of a Deep Learning Predictive Model Combining Clinical and Radiomic Features for Short-Term Postoperative Facial Nerve Function in Acoustic Neuroma Patients*

Meng-yang WANG[1†], Chen-guang JIA[1†], Huan-qing XU[2], Cheng-shi XU[1], Xiang LI[1], Wei WEI[1#], Jin-cao CHEN[1#]
[1]*Department of Neurosurgery, Zhongnan Hospital of Wuhan University, Wuhan 430071, China*
[2]*School of Medical Information Engineering, Anhui University of Chinese Medicine, Hefei 230012, China*

[Abstract] Objective: This study aims to construct and validate a predictable deep learning model associated with clinical data and multi-sequence magnetic resonance imaging (MRI) for short-term postoperative facial nerve function in patients with acoustic neuroma. **Methods:** A total of 110 patients with acoustic neuroma who underwent surgery through the retrosigmoid sinus approach were included. Clinical data and raw features from four MRI sequences (T1-weighted, T2-weighted, T1-weighted contrast enhancement, and T2-weighted-Flair images) were analyzed. Spearman correlation analysis along with least absolute shrinkage and selection operator regression were used to screen combined clinical and radiomic features. Nomogram, machine learning, and convolutional neural network (CNN) models were constructed to predict the prognosis of facial nerve function on the seventh day after surgery. Receiver operating characteristic (ROC) curve and decision curve analysis (DCA) were used to evaluate model performance. A total of 1050 radiomic parameters were extracted, from which 13 radiomic and 3 clinical features were selected. **Results:** The CNN model performed best among all prediction models in the test set with an area under the curve (AUC) of 0.89 (95% CI, 0.84–0.91). **Conclusion:** CNN modeling that combines clinical and multi-sequence MRI radiomic features provides excellent performance for predicting short-term facial nerve function after surgery in patients with acoustic neuroma. As such, CNN modeling may serve as a potential decision-making tool for neurosurgery.
Key words: acoustic neuroma; convolutional neural network; facial nerve function; machine learning; multi-sequence magnetic resonance imaging

Acoustic neuroma (AN) is the most common benign lesion in the posterior cranial fossa, accounting for 80% of all tumors located in the cerebellar pontine angle[1]. Safety and preservation of facial nerve function are the main objectives of surgery[2]. With advanced microscopy, neuronavigation, intraoperative electrophysiological monitoring, and other technologies, complications from resection as well as mortality rates have significantly declined[3]. Many patients express concern about the possibility of postoperative facial paralysis which could have an effect on their social lives. Therefore, improving the prognosis of postoperative facial nerve function with maximum tumor removal is a primary goal.

Meng-yang WANG, E-mail: gzsdxm@163.com; Chen-guang JIA, E-mail: 176281529@qq.com
†The authors contributed equally to this work and share first authorship.
#Corresponding authors, Jin-cao CHEN, E-mail: chenjincao2012@163.com; Wei WEI, E-mail: wei.wei@whu.edu.cn

The facial nerve (FN) is attached to the surface of the acoustic neuroma and, therefore, would be easily damaged during resection. When the mass is severely adherent with the FN, it may lead to poor postoperative FN function[4]. Facial nerve palsy caused by dissecting the FN from the tumor could impair emotional expression and face-to-face communication[5]. FN damage may present as a change of countenance, inability to smile, or trouble moving the lip(s) and/or cheek(s)[6]. Moreover, impairment sometimes takes years or even fails to recover to the preoperative state[7]. Consequently, patients may be forced to disconnect from social life and work, which can cause a severe psychological burden[8–10].

According to current research, 28%–67.1% of patients with acoustic neuroma have an unsatisfied (House-Brackman grade Ⅲ-Ⅵ) short-term (within two weeks after surgery) facial nerve function prognosis[11–13]. Many scholars have analyzed relevant risk factors. Using multivariate logistic regression analysis, Torres *et al* found that medium and large sized, cystic component, strong adhesions between

facial nerves and tumors may be associated with poor prognosis of FN function on day 8 after surgery[14]. However, Taha *et al* proposed that outcome of postoperative facial nerve function may be unrelated to tumor size when CyberKnife (CK) radiosurgery is used as the surgical strategy for majority resection[15]. Differences in previous research outcomes may have resulted from the practice of predicting postoperative FN function based on traditional statistical analysis of clinical variables, which may be improved with an artificial intelligence approach. Alternatively, the variability observed may be due to the subjective assessment of many features, such as the degree of adhesion determined by the neurosurgeon during operation[14]. Meanwhile, objective characteristics are limited to gauging tumor diameter with preoperative MRI[16–17]. In short, previous approaches neglect some important data, such as the intratumor features and three-dimensional information which are hard to perceive. Hence, more innovative and accurate analyses with multiparameters should be introduced.

Deep learning and radiomics have thrived in recent years. These two novel technologies have good clinical application prospects and have been applied to the radiotherapy for acoustic neuroma. Some radiomic models, capable of extracting more subtle and comprehensive characteristics of MRI sequences, are excellent at predicting AN progression[18, 19]. Our research was designed to solve the concerns mentioned above. Here, we explore a well-performing, deep learning model that combines clinical variables and multi-sequence MRI radiomic features to predict short-term postoperative facial nerve function.

1 MATERIALS AND METHODS

1.1 Patients

This study was approved by the Ethics Committee of Zhongnan Hospital of Wuhan University (No. 2021037K), which waived written informed consent. This research was designed in line with the principles of the Declaration of Helsinki. Patients diagnosed with AN (n=110) between June 2018 and October 2022 were enrolled in this study. The inclusion criteria were as follows: 1) all patients with unilateral sporadic AN underwent microsurgery with the assistance of neuronavigation; 2) clinical data, such as gender, age, body mass index (BMI), and short-term facial nerve function after surgery, were complete and collected; 3) all patients underwent MRI scans before surgery and the MRI data were contained at least 4 sequences [T1-weighted (T1W), T2-weighted (T2W), T1-weighted contrast enhancement (T1W+C), and T2-weighted fluid-attenuated inversion recovery (T2-Flair) images]; 4) diagnosis of AN was confirmed by postoperative pathological examination. Patients with incomplete clinical and/or MRI data or neurofibromatosis type Ⅱ were excluded. Short-term FN function was defined according to the outcome of the House-Brackmann (HB) grading system on the seventh day after surgery. HB Ⅰ–Ⅱ define good facial nerve function while HB Ⅲ–Ⅵ define poor. Patients were randomly divided into the training set and test set at a ratio of 7 to 3.

1.2 Parameters of MRI Scan

A total of 4 magnetic resonance sequences were used to provide a broader range of tumor characteristics. T1W+C provided information about blood supply and boundary of the mass. T1W images provide tissue discrimination information. T2W and Flair images provide information like fluid content. MRI was performed with a 3.0-T scanner (uMR790, UIH, China). Parameters of MRI scan included axial T1W (TE, 3.10 ms; TR, 7.24 ms; slice thickness, 1 mm), T2W (TE, 313.56 ms; TR, 2000 ms; slice thickness, 1 mm), and T1W+C using 0.1 mmol/kg gadopentetate dimeglumine (TE, 3.10 ms; TR, 7.24 ms; slice thickness, 1 mm) and T2-Flair (TE, 430.54 ms; TR, 6000 ms; slice thickness, 1 mm).

1.3 Region of Interest Segmentation

Digital Imaging and Communications in Medicine (DICOM) formatted MRI data were analyzed with ITK-SNAP software (Version 3.8.0, PICSL, USA). The region of interest (ROI) included the mass of the AN in the posterior cranial fossa and the part within the internal auditory canal. A senior neurosurgeon manually segmented the ROI and a second experienced doctor assessed the availability. The intraclass correlation coefficient (ICC) was used to evaluate ROI results. Stability and reliability were defined as great when the ICC ≥0.75. Only features with high stability were retained.

1.4 Feature Extraction and Selection

Radiomic features of 4 MRI sequences were extracted using Pyradiomics package implemented in Python (https://pyradiomics.readthedocs.io/en/latest/) and subsequently integrated. These features included the first-order, Gray Level Co-occurrence Matrix (GLCM), Gray Level Dependence Matrix (GLDM), Gray Level Run Length Matrix (GLRLM), Gray Level Size Zone Matrix (GLSZM), Neighboring Gray Tone Difference Matrix (NGTDM), 3-Dimensional Shape, 2-Dimensional Shape, Log Kernel Size, and Wavelet-based feature. Feature selection was performed with clinical variables fused with radiomic features (for machine learning and deep learning models) or with radiomics only (for calculation of Rad score). Features with Spearman correlation coefficient >0.8 were initially retained. The Mann-Whitney U test was used to further screen out features with statistically significant differences (P<0.05). Z-score was used for dimensionless processing of the above data and least absolute shrinkage and selection operator (LASSO)

regression was used to filter the features.

1.5 Model Construction and Validation

Backward step-wised multivariable logistic regression analysis with Akaike Information Criterion (AIC) was used to screen the clinical factors. The Nomogram model was constructed by combining the selected clinical variable and Rad score. Python Scikit-learn (https://scikit-learn.org/stable/) was used to develop several machine learning models, including Support Vector Machine (SVM), Stochastic Gradient Descent (SGD), K-Nearest Neighbor (KNN), Light Gradient Boosting Machine (LightGBM), Decision Tree (DT), Random Forests (RF), Extra Tree (ET) and Logistic Regression (LR). The deep learning model we constructed was a 1D convolutional neural network. Finally, receiver operating characteristic (ROC) curves assessed with the DeLong test and decision curve analysis (DCA) were built to illustrate the area under the curve (AUC) value and net benefits, respectively.

1.6 Statistical Analysis

Python (Version Number: 3.7.0, Python Software Foundation) and R software (Version Number: 4.1.2, R Foundation for Statistical Computing) were used for z-score normalization, Spearman correlation analysis, Mann-Whitney *U* test, LASSO regression analysis, and stepwise regression. The Student *t*-test, Chi-square test, and Fisher test were implemented with SPSS software (Version 22; IBM Corp., USA) to compare continuous and categorical variables. A two-sided $P<0.05$ was considered statistically significant.

2 RESULTS

2.1 Clinical Characteristics

A total of 110 patients were randomly divided into training set (n=77) and test set (n=33). Clinical data, including gender, age, BMI, group (the refined new strategy or the former surgical strategy), tumor size, cerebral spinal fluid (CSF) cap (presence of CSF between the tumor nodule and internal auditory canal fundus on the T2-weighted image), remnant of the tumor, and recurrence cases, were compared between the sets (table 1). These baseline variables had no significant statistical differences between the two sets, except for tumor size.

2.2 Radiomic Signature and Clinical Variables

The segmentation and pipeline of this study are illustrated in fig. 1 and fig. 2, respectively. A total of 1050 radiomic features were extracted for the subsequent analysis process. The LASSO tuned the regular parameter λ using 10-fold cross validation, and the optimized λ was 0.024 (fig. 3).

Selected features for the machine and deep learning processes were age, group, tumor diameter, the original_shape_Maximum2DDiameterRow, original_glszm_LargeAreaLowGrayLevelEmphasis, 3D_firstorder_Entropy, 3D_glszm_LargeAreaLowGrayLevelEmphasis, wavelet-LHH_glszm_ZonePercentage, wa-

Table 1 Clinical characteristics of patients

Characteristics	House-Brackmann grade		Overall (n=110)	P-value
	Good (n=83)	Poor (n=27)		
Gender (n, %)				0.89
Male	32 (38.55)	10 (37.04)	42 (38.18)	
Female	51 (61.45)	17 (62.96)	68 (61.82)	
Age (years), Mean±SD	52±9.92	47.6±10.4	50.9±10.2	0.06
Duration (days), Mean±SD	429±691	356±453	411±640	0.53
Tumor location (%)				0.92
Left side	44 (53.01)	14 (51.85)	58 (52.73)	
Right side	39 (46.99)	13 (48.15)	52 (47.27)	
BMI (kg/m^2), Mean±SD	22.6±2.59	23.5±3.72	22.8±2.92	0.25
Group (n, %)				0.21
New strategy	39 (46.99)	9 (33.33)	48 (43.64)	
Former strategy	44 (53.01)	18 (66.67)	62 (56.36)	
Diameter (mm), Mean±SD	28.0±9.17	35.9±8.28	30.3±9.46	<0.01
CSF Cap (n, %)				0.38
Yes	15 (18.07)	7 (25.93)	22 (20)	
No	68 (81.93)	20 (74.07)	88 (80)	
Recurrence (n, %)				0.99
Yes	2 (2.41)	1 (3.7)	3 (2.73)	
No	81 (97.59)	26 (96.3)	107 (97.27)	
Tumor remnant (n, %)				0.18
Yes	2 (2.41)	3 (11.11)	5 (4.55)	
No	81 (97.59)	24 (88.89)	105 (95.45)	

BMI: body mass index; Cap: signal for cerebral spine fluid (CSF) between the tumor and internal auditory canal fundus on T2-weighted image. Good: House-Brackmann grade Ⅰ–Ⅱ; Poor: House-Brackmann grade Ⅲ–Ⅳ; Duration: the time from the appearance of symptoms to the diagnosis of acoustiv neuvoma

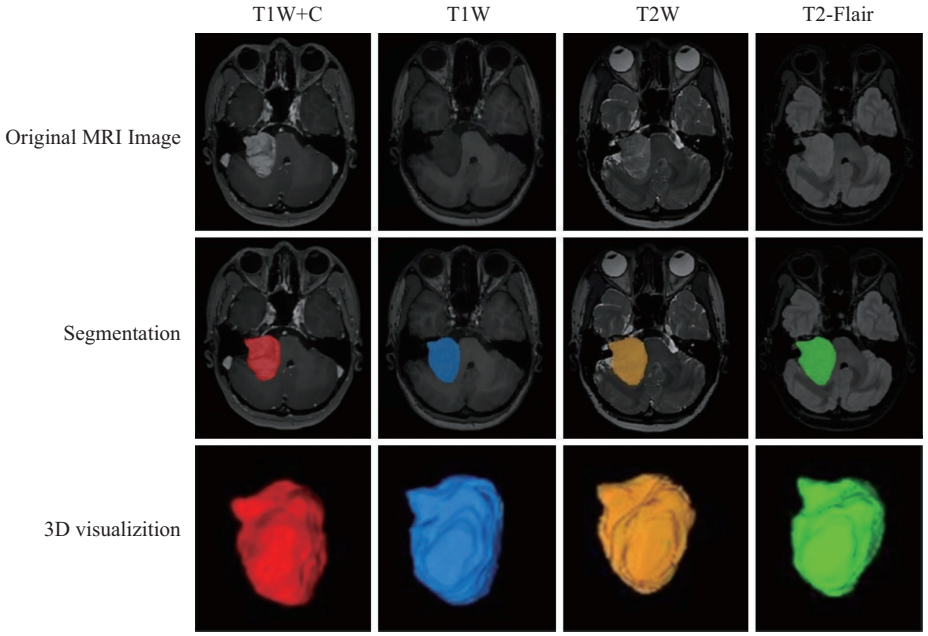

Fig. 1 Region of interest (ROI) segmentation
A total of 4 MRI sequences data processed with ITK-SNAP software (Version 3.8.0, PICSL, USA). ROI is marked red with T1W+C, blue with T1W, yellow with T2W and green with T2-Flair. T1W: T1 weighted; T2W: T2-weighted; T1W+C: T1-weighted contrast enhancement; T2-Flair: T2-weighted fluid-attenuated inversion recovery

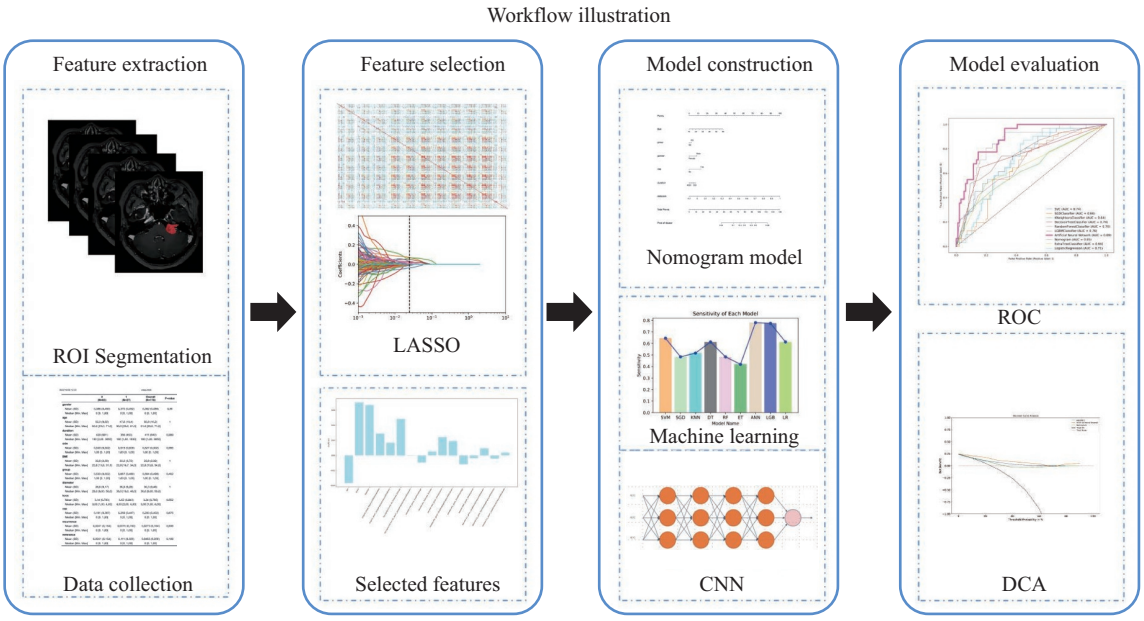

Fig. 2 Workflow of our research
Step 1: Radiomic features were extracted from MRI sequences and clinical data were collected from the hospital. Step 2: Spearman correlation analysis and least absolute shrinkage and selection operator (LASSO) regression were used to select fused clinical and radiomic features. Step 3: Nomogram, machine learning models, and a convolutional neural network (CNN) model were constructed. Step 4: Receiver operating characteristic curve (ROC) and decision curve analysis (DCA) were used to evaluate performance of the models.

velet-HLL_firstorder_Entropy, wavelet-HLH_glszm_ZoneVariance, wavelet-HHL_glszm_SmallAreaHighGrayLevelEmphasis, wavelet-HHL_glszm_ZonePercentage, wavelet-HHH_glszm_ZoneVariance, wavelet-LLL_glrlm_LongRunLowGrayLevelEmphasis, wavelet-LLL_glrlm_ShortRunHighGrayLevelEmphasis, and wavelet-LLL_glszm_LargeAreaLowGrayLevelEmphasis.

2.3 Performance of Different Model

The nomogram model was evaluated by calibration curve (fig. 4 and 5). AUC values in the test and training sets were 0.85 (95% CI: 0.74–0.87) and 0.86 (95% CI: 0.78–0.88), respectively. Among the constructed machine learning models, the LightGBM

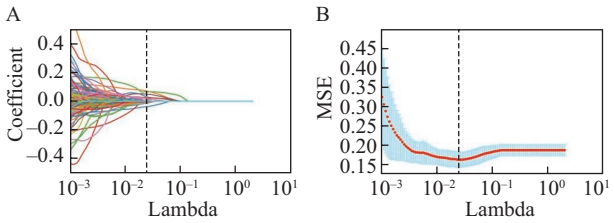

Fig. 3 Lamda value selection for LASSO regression
A: The LASSO tuned the regular parameter λ using 10-fold cross-validation. Optimal λ was 0.024. B: illustration of mean square error (MSE) changes with the LASSO method.

model performed best at predicting the prognosis of FN function on the 7th day after surgery. AUC values in the test and training sets were 0.76 (95% CI: 0.72–0.85) and 0.82 (95% CI: 0.67–0.84), respectively. Model result are presented in table 2. Convolutional neural network (CNN) modeling (fig. 6) resulted in AUC values of 0.89 (95% CI: 0.84–0.91) and 0.95 (95% CI: 0.87–0.98) in the test and the training sets, respectively. In the test set, the CNN model had an accuracy of 81%, a sensitivity of 78%, and a specificity of 87%. In the training set, the CNN had an accuracy of 78%, a sensitivity of 90%, and a specificity of 80% (table 2). Decision curve analysis revealed that, among all 3 models, CNN achieved the highest net benefit (fig. 7). The results show that CNN based on clinical and multi-sequence MRI features may be a reliable method to predict postoperative FN function in patients with AN (fig. 8).

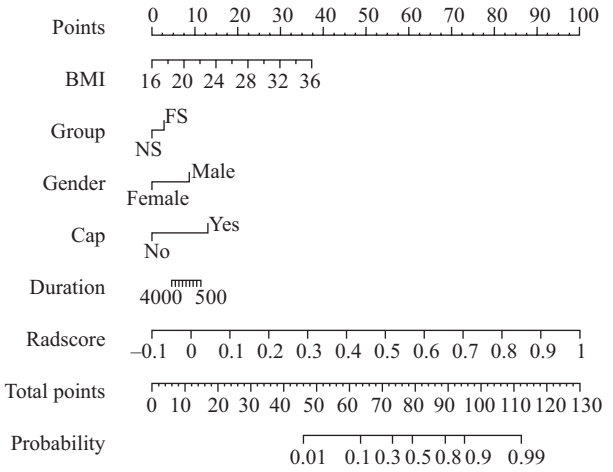

Fig. 4 Illustration of the nomogram
BMI: body mass index; Cap: signal for cerebral spinal fluid between the tumor and internal auditory canal fundus on the T2-weighted image; FS: former strategy for tumor resection; NS: newly refined strategy of tumor resection; Duration: the time from the appearance of symptoms to the diagnosis of acoustic neuroma

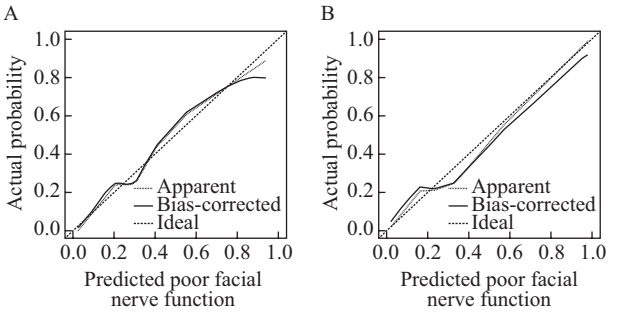

Fig. 5 Calibration curves of the nomogram
A: test set; B: training set

3 DISCUSSION

Our research shows that the CNN model has the best prediction performance. Meanwhile, our study differs from previous articles by using 4 MRI sequences to add more radiomic features instead of employing one single contrast enhancement sequence. We also combined clinical features with the final CNN model construction to improve accuracy. To our knowledge, this is the first study to apply a deep learning model, machine learning models, and the Nomogram model to predict the short-term postoperative outcomes of facial nerve function in patients with AN. Our results show that it is feasible to use the novel algorithm to provide valuable information for neurosurgeons in decision-making. Besides, when patients come for consultation, they can get more details and make adequate physical and psychological preparation for surgery.

Radiomics is a new analysis method that can be used in predictive models for treatment and prognosis[20, 21]. The characteristics of the tumor on the MRI can be quantified and, with subsequent data analysis, redundant and irrelevant information can be removed to obtain more suitable features or independent variables[22, 23]. In recent years, such technologies have been introduced in neurosurgery for clinical decision-making and diagnosis with MRI imaging. Langenhuizen *et al* showed the feasibility of a machine learning model for predicting the long-term stereotactic radiosurgery treatment response of AN using radiomic tumor texture features[24]. This can be helpful for a clinical decision support system and help patients choose the most suitable treatment strategy. Lee *et al* studied multi-sequence MRI images of 516 patients with AN from the Gamma Knife radiosurgery planning system. They constructed an end-to-end deep learning model with U-Net architecture to segment anisotropic MRI images effectively and rapidly[25]. Our research confirms that combining radiomic signatures and clinical variables can be reliably applied to predict the prognosis of postoperative facial nerve function. Our constructed model can efficiently predict FN function because it contains wealthy radiomic characteristics that provide subtle and quantitative features of tumor components, cystic or solid mass. The cystic component of AN is currently universally recognized as an essential risk factor for poor FN function. The cystic form indicates a greater chance of adhesion to

Table 2 Performance of all models

Models	Accuracy		Sensitivity		Specificity		Precision		AUC (95%CI)	
	Test	Training	Test	Training	Test	Training	Test	Training	Test	Training
CNN	0.81	0.78	0.78	0.90	0.87	0.80	0.84	0.93	0.89 (0.84–0.91)	0.95 (0.87–0.98)
Nomogram	0.80	0.63	0.75	0.73	0.83	0.58	0.81	0.91	0.85 (0.74–0.87)	0.86 (0.78–0.88)
LightGBM	0.80	0.73	0.77	0.87	0.81	0.65	0.78	0.83	0.76 (0.72–0.85)	0.82 (0.67–0.84)
SVM	0.65	0.63	0.65	0.86	0.65	0.50	0.69	0.76	0.74 (0.64–0.77)	0.85 (0.82–0.87)
SGD	0.57	0.63	0.48	0.87	0.60	0.50	0.67	0.75	0.66 (0.65–0.71)	0.89 (0.81–0.91)
KNN	0.62	0.62	0.52	0.80	0.66	0.54	0.60	0.72	0.64 (0.61–0.75)	0.83 (0.76–0.90)
Decision tree	0.80	0.61	0.61	0.60	0.85	0.62	0.78	0.86	0.74 (0.66–0.78)	0.75 (0.71–0.80)
Random forest	0.77	0.73	0.48	0.80	0.86	0.69	0.82	0.89	0.70 (0.68–0.75)	0.82 (0.75–0.88)
Extra trees	0.73	0.76	0.42	0.73	0.83	0.77	0.70	0.83	0.66 (0.62–0.76)	0.72 (0.62–0.74)
Logistic regression	0.69	0.68	0.61	0.86	0.72	0.58	0.75	0.88	0.71 (0.66–0.73)	0.83 (0.72–0.88)

CNN: convolutional neural network; KNN: K-nearest neighbor; LightGBM: Light Gradient Boosting Machine; SGD: stochastic gradient descent; SVM: support vector machine

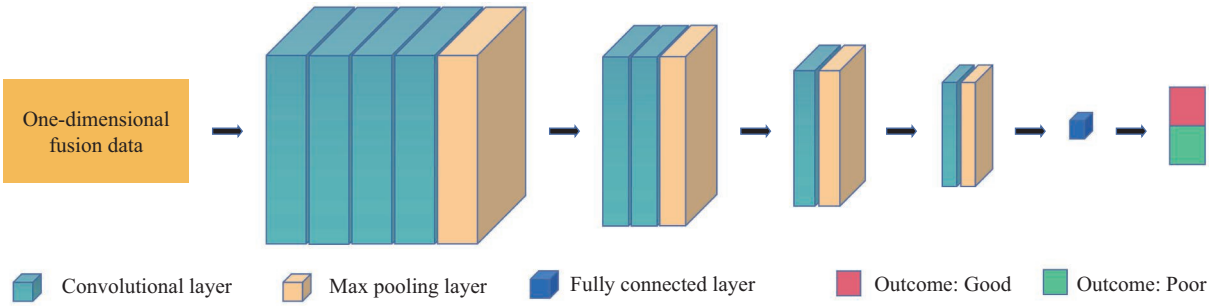

Fig. 6 Workflow for convolutional neural network
The 1D convolutional neural network was constructed as illustrated.

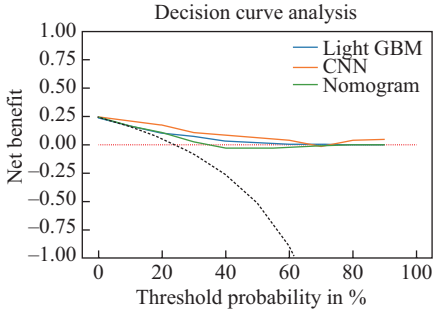

Fig. 7 Decision curve analysis for three models
Yellow line represents the convolutional neural network model which significantly outperformed the other two. Blue line represents the LightGBM model which had the best area under the curve of all machine learning models. Green line represents the nomogram.

the facial nerve and may result in inadvertent damage to FN when dissecting the tumor[26, 27]. However, in clinical studies, the differentiation of cystic AN is subjectively determined by neurosurgeons based on review of MRI images rather than with a quantitative tool to evaluate the composition[13, 28]. Radiomics has the potential to solve the problem. Yang *et al* extracted 1763 radiomic features from multiparametric MRI data. The screened quantified radiomic features indicated the heterogeneous and cystic types relating to the pseudoprogression and long-term outcome of AN after Gamma Knife radiosurgery[18]. Most artificial intelligence (AI) models show a higher degree of accuracy in interpreting contrast-enhanced lesions

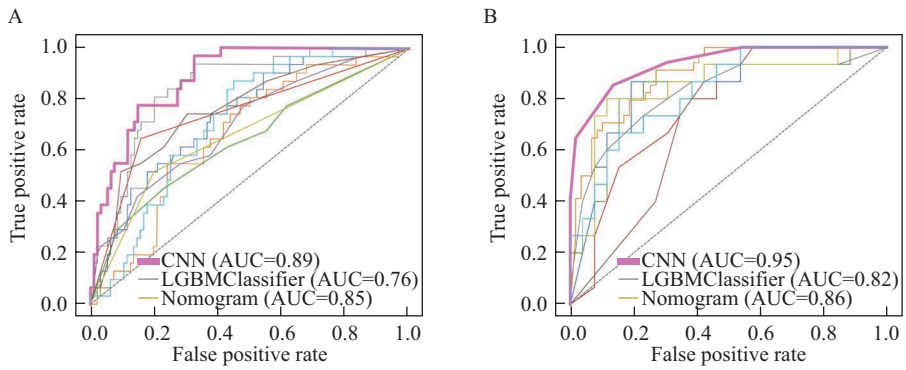

Fig. 8 ROC curves for all models
A: test set; B: training set. The CNN model outperformed all other algorithms. CNN: convolutional neural network; ROC: receiver operating characteristics

versus the cystic component of the tumor. Lee *et al* proposed an AI model to overcome these limitations by combing the sequences with T2W and T1W+C images. This multi-sequence approach makes it possible to precisely evaluate tumor characteristics during the treatment of cystic AN or tumors with loss of significant enhancement[29]. Our results show that multi-sequence MRI radiomics combined with deep learning algorithms can produce a model with great accuracy for FN function prediction, saving time when differentiating tumor components and facilitating decision making. Another possible reason for the excellent performance of our model is that we have contained intratumor heterogeneity, such as adhesion between the tumor capsule and facial nerve. The degree of adhesion is a universally acknowledged critical risk factor of poor FN function[30]. Nonetheless, there are two problems with determining the adhesive degree: 1) identification criterion is so objective and different as it mainly depends on observation by the neurosurgeon with naked eyes during surgery[31] and 2) the FN is almost integrated anatomically with the mass as a wholly enhanced lesion on MRI, leaving unrecognizable intraoperative dissection plane[32]. However, the ROI delineation can segment the entire enhanced lesion with integrated FN. Therefore, adhesion of the facial nerve is transformed into heterogeneity inside the tumor which can be interpreted with first-order or high-order radiomic features. Liu *et al* suggested that selected radiomics, GLCM, GLSZM, GLRLM, and first order features, can explain tumor characteristics, intratumor heterogeneity, and subtle alterations in tissue morphology[19]. George-Jones *et al* further expanded the application of radiomics to the protein level by presenting that several commonly adopted high-order radiomic features, such as GLCM, are associated with intratumor histology[33]. In our research, both first-order and high-order features are included. The first-order Entropy reflects the first-order feature, GLSZM and GLRLM reflect high-order features, and the Maximum2DDiameterRow reflects the shape. By verifying the performance of the CNN model, we confirmed that the radiomic features containing the important characteristic information could better reflect the FN prognosis.

Deep learning combined with radiomics is also a prevalent approach with excellent accuracy employed by many scholars to solve clinical problems. Zhang *et al* used clinical data and pre-treatment high-resolution thoracic CT to build a convolutional neural network to analyze 720 solid pulmonary nodules. They concluded that the radiomics and deep learning models were well-performing and predictable tools for malignancy of solid pulmonary nodules[34]. Lin *et al* showed that a jointly constructed model with all clinical, conventional radiomic, and deep learning features had a great accuracy for predicting a good pathological response (GPR) in non-small cell lung cancer (NSCLC) patients receiving immunotherapy-based neoadjuvant therapy (NAT)[35]. Our novel approach makes analyzing the inherent connections between variables and outcomes easier, thereby improving the model's accuracy. Since adopting deep learning algorithms based on radiomics, the reliability and accuracy of our research have improved.

There are indeed some limitations to our research. First, this is a retrospective study with inherent bias and limitations. Second, although we used the characteristics of four MRI sequences to expand the number of radiomic features, a larger sample size study is needed to verify relevant models. Finally, multi-center data sets and external verification are needed to further corroborate the results of this study.

To sum up, our deep learning predictive model combining clinical and radiomic features for short-term postoperative FN function in patients with acoustic neuroma has excellent predictive ability. Our model could serve as a potential decision-making tool to assist neurosurgeons in adjusting treatment strategy.

Acknowledgments

We sincerely thank artificial intelligence engineer, Huan-qing XU, for providing important support for our machine and deep learning algorithms as well as data analysis.

Conflict of Interest Statement

The authors declare no conflicts of interest.

REFERENCES

1 Koike H, Morikawa M, Ishimaru H, *et al*. Quantitative Chemical Exchange Saturation Transfer Imaging of Amide Proton Transfer Differentiates between Cerebellopontine Angle Schwannoma and Meningioma: Preliminary Results. IJMS, 2022,23(17):10187

2 Egiz A, Nautiyal H, Alalade AF, *et al*. Evaluating growth trends of residual sporadic vestibular schwannomas: a systematic review and meta-analysis. J Neurooncol, 2022,159(1):135-150

3 Yaşargil MG. The internal acoustic meatus. J Neurosurg, 2002,97(5):1014-1017

4 Jung GS, Montibeller GR, Fraga GS de, *et al*. Facial Nerve Adherence in Vestibular Schwannomas: Classification and Radiological Predictors. J Neurol Surg B Skull Base, 2020,82(4):456-460

5 Fishman Z, Kiss A, Zuker RM, *et al*. Measuring 3D facial displacement of increasing smile expressions. J Plast Reconstr Aesthet Surg, 2022,75(11):4273-4280

6 Bali ZU, Tuluy Y, Özkaya Ünsal M, *et al*. The evaluation of the effect of free gracilis muscle transfer on cheek tone and oral competence in long-standing facial paralysis of patients by using Blasco index. Microsurgery, Online ahead of print. October 19, 2022:micr.30976

7 Khan NR, Elarjani T, Jamshidi AM, *et al*. Microsurgical Management of Vestibular Schwannoma (Acoustic Neuroma): Facial Nerve Outcomes, Radiographic

Analysis, Complications, and Long-Term Follow-Up in a Series of 420 Surgeries. World Neurosurg, 2022,168:e297-e308
8 Osthues M, Kuttenreich AM, Volk GF, *et al*. Continual rehabilitation motivation of patients with postparalytic facial nerve syndrome. Eur Arch Otorhinolaryngol, 2022,279(1):481-491
9 Pattinson R, Poole HM, Shorthouse O, *et al*. Exploring beliefs and distress in patients with facial palsies. Psychol Health Med, 2022,27(4):788-802
10 Cross T, Sheard CE, Garrud P, *et al*. Impact of facial paralysis on patients with acoustic neuroma. Laryngoscope, 2000,110(9):1539-1542
11 Huang X, Xu J, Xu M, *et al*. Functional outcome and complications after the microsurgical removal of giant vestibular schwannomas via the retrosigmoid approach: a retrospective review of 16-year experience in a single hospital. BMC Neurol, 2017,17(1):18
12 Hiruta R, Sato T, Itakura T, *et al*. Intraoperative transcranial facial motor evoked potential monitoring in surgery of cerebellopontine angle tumors predicts early and late postoperative facial nerve function. Clin Neurophysiol, 2021,132(4):864-871
13 Mastronardi L, Gazzeri R, Barbieri FR, *et al*. Postoperative Functional Preservation of Facial Nerve in Cystic Vestibular Schwannoma. World Neurosurg, 2020,143:e36-e43
14 Torres R, Nguyen Y, Vanier A, *et al*. Multivariate Analysis of Factors Influencing Facial Nerve Outcome following Microsurgical Resection of Vestibular Schwannoma. Otolaryngol Head Neck Surg, 2017,156(3):525-533
15 Taha I, Hyvärinen A, Ranta A, *et al*. Facial nerve function and hearing after microsurgical removal of sporadic vestibular schwannomas in a population-based cohort. Acta Neurochir, 2020,162(1):43-54
16 Saleh E, Piccirillo E, Migliorelli A, *et al*. Wait and Scan Management of Intra-canalicular Vestibular Schwannomas: Analysis of Growth and Hearing Outcome. Otol Neurotol, 2022,43(6):676-684
17 Carlstrom LP, Muñoz-Casabella A, Perry A, *et al*. Dramatic Growth of a Vestibular Schwannoma After 16 Years of Postradiosurgery Stability in Association With Exposure to Tyrosine Kinase Inhibitors. Otol Neurotol, 2021,42(10):e1609-e1613
18 Yang HC, Wu CC, Lee CC, *et al*. Prediction of pseudoprogression and long-term outcome of vestibular schwannoma after Gamma knife radiosurgery based on preradiosurgical MR radiomics. Radiother Oncol, 2021,155:123-130
19 Liu J, Sun D, Chen L, *et al*. Radiomics Analysis of Dynamic Contrast-Enhanced Magnetic Resonance Imaging for the Prediction of Sentinel Lymph Node Metastasis in Breast Cancer. Front Oncol, 2019,9:980
20 Zhang Z, Li X, Sun H. Development of machine learning models integrating PET/CT radiomic and immunohistochemical pathomic features for treatment strategy choice of cervical cancer with negative pelvic lymph node by mediating COX-2 expression. Front Physiol, 2022,13:994304
21 Zhu F, Zhu Z, Zhang Y, *et al*. Severity detection of COVID-19 infection with machine learning of clinical records and CT images. Technol Health Care, 2022,30(6):1299-1314
22 Zeng Q, Li H, Zhu Y, *et al*. Development and validation of a predictive model combining clinical, radiomics, and deep transfer learning features for lymph node metastasis in early gastric cancer. Front Med, 2022,9:986437
23 Yang H, Yan S, Li J, *et al*. Prediction of acute versus chronic osteoporotic vertebral fracture using radiomics-clinical model on CT. Eur J Radiol, 2022,149:110197
24 Langenhuizen PPJH, Zinger S, Leenstra S, *et al*. Radiomics-Based Prediction of Long-Term Treatment Response of Vestibular Schwannomas Following Stereotactic Radiosurgery. Otol Neurotol, 2020,41(10): e1321-e1327
25 Lee WK, Wu CC, Lee CC, *et al*. Combining analysis of multi-parametric MR images into a convolutional neural network: Precise target delineation for vestibular schwannoma treatment planning. Artif Intell Med, 2020,107:101911
26 Boublata L, Belahreche M, Ouchtati R, *et al*. Facial Nerve Function and Quality of Resection in Large and Giant Vestibular Schwannomas Surgery Operated By Retrosigmoid Transmeatal Approach in Semi-sitting Position with Intraoperative Facial Nerve Monitoring. World Neuros, 2017,103:231-240
27 Link MJ, Driscoll CLW, Feng Y, *et al*. Retrosigmoid Approach for Resection of Large Cystic Vestibular Schwannoma. J Neurol Surg B. 2019,80(S 03):S285-S285
28 Moon KS, Jung S, Seo SK, *et al*. Cystic vestibular schwannomas: a possible role of matrix metalloproteinase–2 in cyst development and unfavorable surgical outcome. JNS, 2007,106(5):866-871
29 Lee CC, Lee WK, Wu CC, *et al*. Applying artificial intelligence to longitudinal imaging analysis of vestibular schwannoma following radiosurgery. Sci Rep, 2021,11(1):3106
30 Mastronardi L, Campione A, Boccacci F, *et al*. Koos grade IV vestibular schwannomas: considerations on a consecutive series of 60 cases—searching for the balance between preservation of function and maximal tumor removal. Neurosurg Rev, 2021,44(6):3349-3358
31 Liu C, Shen Y, Han D, *et al*. Analysis of Related Factors Affecting Facial Nerve Function after Acoustic Neuroma Surgery. Evid Based Complement Alternat Med, 2022,2022:1-6
32 Elsayed M, Jia H, Hochet B, *et al*. Intraoperative facial nerve electromyography parameters to optimize postoperative facial nerve outcome in patients with large unilateral vestibular schwannoma. Acta Neurochir, 2021,163(8):2209-2217
33 George-Jones NA, Chkheidze R, Moore S, *et al*. MRI Texture Features are Associated with Vestibular Schwannoma Histology. Laryngoscope, 2021,131(6):E2000-E-2006
34 Zhang R, Wei Y, Shi F, *et al*. The diagnostic and prognostic value of radiomics and deep learning technologies for patients with solid pulmonary nodules in chest CT images. BMC Cancer, 2022,22(1):1118
35 Lin Q, Wu HJ, Song QS, *et al*. CT-based radiomics in predicting pathological response in non-small cell lung cancer patients receiving neoadjuvant immunotherapy. Front Oncol, 2022,12:937277

(Received Nov. 15, 2022; accepted Jan. 14, 2023)